

Thermodynamics of Non-linear magnetic-charged AdS black hole surrounded by quintessence, in the background of perfect fluid dark matter

Ragil Brand Ndongmo^{1,*}, Saleh Mahamat², Thomas Bouetou Bouetou^{1,3}, Conrad Bertrand Tabi⁴, Timoleon Crepin Kofane^{1,4}

1 Department of Physics, Faculty of Science, University of Yaounde I, P.O. Box. 812, Yaounde, Cameroon,

2 Department of Physics, Higher Teacher's Training College, University of Maroua, P.O. Box 55, Maroua, Cameroon,

3 National Advanced School of Engineering, University of Yaounde I, P.O. Box. 8390, Yaounde, Cameroon,

4 Department of Physics and Astronomy, Botswana International University of Science and Technology, Private Mail Bag 16, Palapye, Botswana

* nragilbrand@gmail.com

Abstract

In this paper, we study the thermodynamic features of a non-linear magnetic-charged AdS black hole surrounded by quintessence, in the background of perfect fluid dark matter(PFDM). After having obtained the corresponding metric, we put out the mass and the temperature of the black hole, in order to get its entropy. Subsequently, we find the expression of the pressure which leads us to get the table of critical values and the isothermal diagram. Especially, we find that the critical values of the temperature and the pressure increase as the dark matter parameter increases. Also, analysing the isothermal diagram, we observe a van der Waals-like behaviour remarked by the presence of a first-order phase transition when we cross the critical temperature. Additionally, we compute and plot the heat capacity of the black hole and find that a second-order phase transition occurs, leading the black hole to move from a stable phase to an unstable one. Furthermore, it comes out that this phase transition point is shifted towards higher values of the horizon radius, as we decrease the dark matter density and increase the quintessence density.

1 INTRODUCTION

The thermodynamic study of black holes is one of the most used way to apprehend black holes since the seminal works of Hawking [1] and Bekenstein [2]. Precisely, they found outstanding results such that black holes radiate as black bodies. In this way, we could find many thermodynamic quantities of the black hole, namely the temperature, the entropy, the volume, the heat capacity, and so on [3–6]. Since then, many works have been done on the thermodynamics of black holes [7–16].

One of the properties of black holes predicted by the Einstein theory of general relativity is known as Singularity, which is the point of space-time for which the predictive physical laws are broken down [17, 18]. In order to solve this problem, many alternative solutions without singularity have been constructed and they are called regular black holes. The Bardeen black hole belongs to these solutions [15, 19, 20], with an event horizon satisfying the weak energy condition. It has been derived by introducing an energy-momentum tensor, interpreted as the gravitational field of some sort of a non-linear magnetic monopole charge Q . Thereby, many authors have been interested in these regular black holes and their geometrical and thermodynamic properties [21–25].

A recent fascinating results of observational cosmology is the accelerated expansion of the Universe [26–28]. Moreover, this result has been confirmed by the measurement of the Cosmic Microwave Background (CMB) by the PLANCK space Satellite [29]. To explain such a phenomenon, an exotic scalar field with a large negative pressure called "dark energy" has been suggested as being the major component, up to 70% of the total energy of the Universe [7]. Many candidates have been proposed to be dark energy. A well known of them is the cosmological constant. Beside it, the model used by many authors is called quintessence, which is characterised by a parameter ϵ , defined as the ratio of the pressure to the energy density of the dark energy. ϵ is defined in the range $-1 < \epsilon \leq -\frac{1}{3}$ [7, 11, 30]. Therefore, it seems interesting to study the effects of quintessence on black holes. In that way, Kiselev [31] has proposed a solution corresponding to the Schwarzschild black hole surrounded by the quintessence. Afterwards, many works have been done in order to study the black hole in the quintessence field [9, 10, 32–38].

Beside dark energy, another unsolved problem in cosmology and astrophysics is dark matter, which constitutes about 23% of the total mass-energy of the universe [39], according to the Standard Model of Cosmology. Many theoretical models have been proposed to be dark matter. Beside Cold Dark Matter (CDM) [40], Warm Dark Matter [41, 42] and Scalar Field Dark Matter [43, 44], the Perfect fluid dark matter(PFDM) is one among them, and it has been shown that the PFDM can explain the asymptotically flat rotation curves concerning spiral galaxies [45]. Hence, the PFDM has been introduced in many works concerning black holes [46–49].

Since seminal work of Hawking and Page [50], it has been shown that black holes undergo to a phase transition, in the AdS/CFT correspondence. Furthermore, the understanding of the phase transition could be extended to the one between small-large black hole, as it is shown by many authors [51–53], for which they shown a complete analogy with the van der Waals liquid-gas system. A better result can be obtained by considering the cosmological constant as a dynamical pressure and its conjugate quantity as a thermodynamic volume in the extended phase space [54–62]. Another way to study the black hole phase transitions is through the behaviour of its heat capacity [7]. Especially, Husain and Mann [14] suggested that the specific heat of a black hole becomes positive after a phase transition near the Planck scale, and the presence of a discontinuity in the plot of the heat capacity shows the presence of a second-order phase transition. Afterwards, many author used this method in order to explore the black hole phase transition(see [7, 15, 63–67]). Especially, Nam [68] derived a non-linear magnetic-charged black hole surrounded by quintessence, and studied its thermodynamic stability. As a result, he found that the black hole may undergo, at a critical temperature, a thermal phase transition, between a larger unstable black hole and a smaller stable black hole. Therefore, what could we have if we also take into account the presence of dark matter, in the AdS space-time?

In this paper, motivated by the astrophysical observations and theoretical proposals of dark energy and dark matter, we aim at studying the impact of these two components on the thermodynamic behaviour of the non-linear magnetic-charged AdS black hole.

The paper is organised as follows. In the next section, we derive the metric corresponding to the non-linear magnetic-charged AdS black hole surrounded by quintessence, in the background of perfect fluid dark matter. In section 3, by considering the cosmological constant acting as a dynamical pressure, we study the thermodynamic stability and the phase transitions of the black hole and we put out the effects of the dark energy and the PFDM in the background of the non-linear magnetic-charged AdS black hole. The last section is devoted to the conclusion.

2 NON-LINEAR MAGNETIC-CHARGED AdS BLACK HOLE SURROUNDED BY QUINTESSENCE AND THE PERFECT FLUID DARK MATTER

In the presence of quintessence, the action corresponding to the Einstein gravity coupled to a non-linear electromagnetic field in the four-dimensional AdS space-time and in the presence of PFDM

can be expressed as [39, 69–74]

$$S = \int d^4x \sqrt{-g} \left[\frac{1}{16\pi} \left(R - 2\Lambda - 4\pi \mathcal{L}_{\text{PDFM}} + \mathcal{L}_{\text{quint}} \right) - \frac{1}{4\pi} \mathcal{L}(F) \right], \quad (1)$$

where R is the scalar curvature, Λ is the cosmological constant, $\mathcal{L}(F)$ is the non-linear electrodynamic term and is a function of the invariant $F_{\mu\nu}F^{\mu\nu}/4 \equiv F$, with $F_{\mu\nu} = \partial_\mu A_\nu - \partial_\nu A_\mu$, being the field strength of the non-linear electromagnetic field, and A_ν is the gauge potential of the electromagnetic field. The expression $\mathcal{L}(F)$ is given by [68, 75–78]

$$\mathcal{L}(F) = \frac{3M}{|Q|^3} \frac{(2Q^2F)^{3/2}}{\left[1 + (2Q^2F)^{3/4}\right]^2}, \quad (2)$$

where M is the black hole mass and Q the magnetic charge.

The PFDM term in Eq. (1) is remarked by the term $\mathcal{L}_{\text{PDFM}}$, which is the PFDM Lagrangian density, and $\mathcal{L}_{\text{quint}}$ is the term corresponding to quintessence, which is given by [79–81]

$$\mathcal{L}_{\text{quint}} = -\frac{1}{2}(\nabla\phi)^2 - V(\phi), \quad (3)$$

where ϕ is the quintessential scalar field, and $V(\phi)$ is the potential.

Therefore, applying variational principle from Eq. (1), we get the Einstein-Maxwell equations of motion, expressed as follow [68, 82]

$$G_\mu^\nu + \Lambda\delta_\mu^\nu = 2 \left(\frac{\partial \mathcal{L}(F)}{\partial F} F_{\mu\rho} F^{\nu\rho} - \delta_\mu^\nu \mathcal{L}(F) \right) + 8\pi T_\mu^\nu, \quad (4)$$

$$\nabla_\mu \left(\frac{\partial \mathcal{L}(F)}{\partial F} F^{\nu\mu} \right) = 0, \quad (5)$$

$$\nabla_\mu * F^{\nu\mu} = 0. \quad (6)$$

Here, T_μ^ν represents the energy-momentum tensor of both the PFDM and quintessence, which can be expressed as

$$T_\mu^\nu = T_\mu^\nu(\text{PFDM}) - \frac{1}{4\pi} T_\mu^\nu(\text{Quintessence}). \quad (7)$$

Since dark matter is considered as a kind of perfect fluid, the energy-momentum tensor is then written as $T_\mu^\nu = \text{diag}[-\rho, p, p, p]$ [39, 69, 70], with ρ and p being the energy density and the pressure respectively. Furthermore, in the simplest case, we assume $\frac{p}{\rho} = \delta - 1$, where δ is a constant [69].

Now, since we need to find a spherically symmetric space solution in the quintessence and PFDM, the metric has to be written with ansatz [39, 68, 83]

$$ds^2 = -e^\nu dt^2 + e^\lambda dr^2 + r^2(d\theta^2 + \sin^2\theta d\phi^2) \quad (8)$$

$$= -f(r)dt^2 + \frac{1}{f(r)}dr^2 + r^2(d\theta^2 + \sin^2\theta d\phi^2), \quad (9)$$

$$\text{with } f(r) = 1 - \frac{2m(r)}{r} - \frac{\Lambda}{3}r^2. \quad (10)$$

The ansatz we use for the Maxwell field is expressed as [39, 68]

$$F_{\mu\nu} = (\delta_\mu^\theta \delta_\nu^\varphi - \delta_\nu^\theta \delta_\mu^\varphi) B(r, \theta), \quad (11)$$

and the non-linear electrodynamic term is given explicitly as [68]

$$\mathcal{L}(F) = \frac{3M}{|Q|^3} \frac{(2Q^2F)^{\frac{3}{2}}}{\left[1 + (2Q^2F)^{\frac{3}{4}}\right]^2} = \frac{3MQ^3}{(r^3 + Q^3)^2}, \text{ with } F = \frac{Q^2}{2r^4}. \quad (12)$$

Considering the time component of Eq.(4), we get

$$G_t^t + \Lambda \delta_t^t = 2 \left(\frac{\partial \mathcal{L}(F)}{\partial F} F_{t\rho} F^{t\rho} - \delta_t^t \mathcal{L}(F) \right) + 8\pi T_t^t. \quad (13)$$

Now, since the time components of energy-momentum for the PFDM and for quintessence are related to their energy density, we can write the last term of Eq.(13) as follows [82]

$$T_t^t = T_t^t(PFDM) - \frac{1}{4\pi} T_t^t(Quintessence) = \frac{1}{8\pi} \frac{\alpha}{r^3} + \frac{1}{4\pi} \left(\frac{3\epsilon c}{2r^{3(\epsilon+1)}} \right), \quad (14)$$

where α denotes the intensity of the PFDM, c and ϵ are the quintessence parameters.

Therefore, from Eq.(13), we get straightforwardly

$$G_t^t + \Lambda = -2\mathcal{L}(F) + \frac{\alpha}{r^3} + \frac{3\epsilon c}{r^{3(\epsilon+1)}}, \quad (15)$$

since $\delta_t^t = 1$, and $F_{t\rho} F^{t\rho} = 0$.

Before solving Eq.(15), we first have to find the component G_{tt} of the Einstein tensor, which is obtained using the metric Eq.(8), by

$$G_{tt} = e^\nu \left[\frac{1}{r^2} - e^{-\lambda} \left(\frac{1}{r^2} - \frac{\lambda'}{r} \right) \right]. \quad (16)$$

Developing it, we get

$$\begin{aligned} G_{tt} &= f(r) \left[\frac{1}{r^2} - f(r) \left(\frac{1}{r^2} - \frac{1}{r} \left(-\frac{f'(r)}{f(r)} \right) \right) \right], \quad \text{with } \lambda = -\ln f(r) \\ &= f(r) \left[\frac{1}{r^2} - f(r) \left(\frac{1}{r^2} - \frac{1}{rf(r)} \left[2 \left(\frac{m'(r)}{r} - \frac{m(r)}{r^2} + \frac{\Lambda}{3} r^2 \right) \right] \right) \right] \\ &= f(r) \left(\frac{2m'(r)}{r^2} + \Lambda \right). \end{aligned}$$

Therefore, the component G_t^t of Eq.(16) is expressed as

$$G_t^t = g^{tt} G_{tt} = (-f(r))^{-1} f(r) \left(\frac{2m'(r)}{r^2} + \Lambda \right), \quad (17)$$

meaning that

$$G_t^t = -\frac{2m'(r)}{r^2} - \Lambda. \quad (18)$$

Now, replacing Eq.(18) into Eq.(15), we get

$$m'(r) = \frac{3MQ^3r^2}{(r^3 + Q^3)^2} - \frac{\alpha}{2r} - \frac{3\epsilon c}{2r^{3\epsilon+1}}.$$

By integration, we obtain

$$m(r) = -\frac{MQ^3}{r^3 + Q^3} - \frac{\alpha}{2} \ln \frac{r}{|\alpha|} + \frac{c}{2r^{3\epsilon}} + C^{st}. \quad (19)$$

Now, to find the integral constant C^{st} , we will use the boundary condition [68,82]

$$M = \lim_{r \rightarrow \infty} \left\{ m(r) + \frac{\alpha}{2} \ln \frac{r}{|\alpha|} - \frac{c}{2r^{3\epsilon}} \right\} = \lim_{r \rightarrow \infty} \left\{ -\frac{MQ^3}{r^3 + Q^3} + C^{st} \right\},$$

leading to

$$C^{st} = M. \quad (20)$$

Hence, the mass $m(r)$ and the function $f(r)$ are respectively given by

$$m(r) = \frac{Mr^3}{r^3 + Q^3} - \frac{\alpha}{2} \ln \frac{r}{|\alpha|} + \frac{c}{2r^{3\epsilon}}, \quad (21)$$

$$f(r) = 1 - \frac{2Mr^2}{r^3 + Q^3} + \frac{\alpha}{r} \ln \frac{r}{|\alpha|} - \frac{c}{r^{3\epsilon+1}} - \frac{\Lambda}{3}r^2. \quad (22)$$

Hereby, the spherically symmetric solution for the action (1) is obtained as

$$ds^2 = -f(r)dt^2 + \frac{1}{f(r)}dr^2 + r^2(d\theta^2 + \sin^2\theta d\phi^2), \quad (23)$$

with $f(r) = 1 - \frac{2Mr^2}{r^3 + Q^3} + \frac{\alpha}{r} \ln \frac{r}{|\alpha|} - \frac{c}{r^{3\epsilon+1}} - \frac{\Lambda}{3}r^2$.

Let us notice first that if we replace the quintessence parameter $c = 0$ and the cosmological constant $\Lambda = 0$ into Eq.(23), we recover the metric of non-linear magnetic-charged black hole surrounded by dark matter considered by Ma et al. [78]. Now, using the horizon propriety [66, 68], and solving the following equation at the horizon

$$f(r_h) = 0, \quad (24)$$

leads to

$$M = \frac{(r_h^3 + Q^3)}{2r_h^2} \left(1 + \frac{\alpha}{r_h} \ln \frac{r_h}{|\alpha|} - \frac{c}{r_h^{3\epsilon+1}} - \frac{\Lambda}{3}r_h^2 \right). \quad (25)$$

Eq.(25) gives the relation between the black hole mass and its horizon radius.

3 THERMODYNAMIC PHASE TRANSITION

For the next step, we will make the thermodynamic analysis of the black hole. First, we will get the isothermal $P - r_h$ diagram, and to do that, we consider that the cosmological constant term Λ will act as a dynamical pressure. Thus, we could write [54–62]

$$P = -\frac{\Lambda}{8\pi}. \quad (26)$$

Therefore, substituting Λ from Eq.(26) into Eq.(25), we readily find

$$M = \frac{(r_h^3 + Q^3)}{2r_h^2} \left(1 + \frac{\alpha}{r_h} \ln \frac{r_h}{|\alpha|} - \frac{c}{r_h^{3\epsilon+1}} + \frac{8\pi P}{3}r_h^2 \right). \quad (27)$$

The Hawking temperature is found through the surface gravity definition at the horizon [68]

$$T = \frac{\kappa}{2\pi} = \frac{f'(r_h)}{4\pi} = \frac{1}{4\pi} \left\{ -2M \left[\frac{2r_h(r_h^3 + Q^3) - 3r^4}{(r_h^3 + Q^3)^2} \right] - \frac{\alpha}{r_h^2} \ln \frac{r_h}{|\alpha|} + \frac{\alpha}{r_h^2} + \frac{c(3\epsilon+1)}{r_h^{3\epsilon+2}} + \frac{16\pi P}{3}r_h \right\}. \quad (28)$$

Thus, using Eq.(27), Eq.(28) may become as

$$T = \frac{1}{4\pi(r_h^3 + Q^3)} \left[\frac{r_h^3 - 2Q^3}{r_h} + \frac{3c\epsilon}{r_h^{3\epsilon+2}} \left(r_h^3 + Q^3 \left(\frac{\epsilon+1}{\epsilon} \right) \right) + \frac{\alpha Q^3}{r_h^2} \left(1 - 3 \ln \frac{r_h}{|\alpha|} \right) + \alpha r_h + 8\pi P r_h^4 \right]. \quad (29)$$

For $\alpha \approx 0$ and $P = 0$, meaning that in the absence of dark matter and cosmological constant, we find the Hawking temperature of the non-linear magnetic-charged black hole surrounded by quintessence which has been obtained by Nam [68], given by

$$T = \frac{1}{4\pi(r_h^3 + Q^3)} \left[\frac{r_h^3 - 2Q^3}{r_h} + \frac{3c\epsilon}{r_h^{3\epsilon+2}} \left(r_h^3 + Q^3 \left(\frac{\epsilon+1}{\epsilon} \right) \right) \right]. \quad (30)$$

The entropy is obtained from the temperature and mass, through the relation

$$S = \int \frac{1}{T} \frac{\partial M}{\partial r_h} dr_h. \quad (31)$$

From Eq.(27), we have obtained the first derivative of the mass with respect to the horizon radius as

$$\frac{\partial M}{\partial r_h} = \frac{1}{2r^2} \left[\frac{r_h^3 - 2Q^3}{r_h} + \frac{3c\epsilon}{r_h^{3\epsilon+2}} \left(r_h^3 + Q^3 \left(\frac{\epsilon+1}{\epsilon} \right) \right) + \frac{\alpha Q^3}{r_h^2} \left(1 - 3 \ln \frac{r_h}{|\alpha|} \right) + \alpha r_h + 8\pi P r_h^4 \right]. \quad (32)$$

Hence, using Eq.(31), we straightforwardly obtain the entropy of the black hole as

$$S = \pi r_h^2 \left(1 - \frac{2Q^3}{r_h^3} \right). \quad (33)$$

Now, the next step consists of deriving the expression of the pressure P as a function of T and r_h , then ending by analysing the critical behaviour of $P - r_h$ diagram.

From Eq. (29), one can explicitly express the pressure P as a function of T and r_h as

$$P = \frac{1}{8\pi r_h^4} \left[4\pi(r_h^3 + Q^3)T - \frac{r_h^3 - 2Q^3}{r_h} - \frac{3c\epsilon}{r_h^{3\epsilon+2}} \left(r_h^3 + Q^3 \left(\frac{\epsilon+1}{\epsilon} \right) \right) - \frac{\alpha Q^3}{r_h^2} \left(1 - 3 \ln \frac{r_h}{|\alpha|} \right) - \alpha r_h \right]. \quad (34)$$

Since the black hole mass M is most naturally associated with the enthalpy H of the black hole in the extended phase space [66], the expression of the volume can be expressed as follows

$$V = \left(\frac{\partial H}{\partial P} \right)_{r_h, Q} = \left(\frac{\partial M}{\partial P} \right)_{r_h, Q} = \frac{4}{3}\pi(r_h^3 + Q^3). \quad (35)$$

α	r_{h_c}	T_c	P_c
0.01	2.7109	0.0126	0.0032
0.05	2.7546	0.0127	0.0032
0.1	2.7756	0.0132	0.0033
0.2	2.7763	0.0148	0.0034
0.4	2.7090	0.0190	0.0039
0.6	2.5947	0.0240	0.0045
0.8	2.4418	0.0308	0.0054

Table 1. Critical values for $(Q, c, \epsilon) = (1, 0.2, -2/3)$ for different dark matter parameters α .

However, given that the expression of pressure would be less complex if we express it in term of horizon radius rather than volume, we will make our thermodynamic analysis with the isothermal $P - r_h$ diagram. Therefore, we putted out in Table 1 critical values which lead us to have an inflexion point in the isothermal $P - r_h$ diagram. They are found through the following system of equations

$$\left(\frac{\partial P}{\partial r_h} \right)_T = 0, \quad \left(\frac{\partial^2 P}{\partial r_h^2} \right)_T = 0. \quad (36)$$

Next, we investigate Eq.(36) numerically in order to get the Table 1, since it is not a trivial task to solve it analytically.

Therefore, it is shown in the present calculation(see Table 1) the impact of PFDM on the critical values. remarkably, we can notice that when increasing the PFDM parameter α , we see that r_{h_c} increases for $\alpha < 0.2$ and then decreases when $\alpha > 0.2$. At the same time, we notice that T_c and P_c increase as we increase α .

In Fig. 1, we plotted the $P - r_h$ diagram. Analysing this plot, we observe a van der Waals like behaviour. This means that a first-order phase transition occurs, moving from $T < T_c$ to $T > T_c$. Here, the first region($T < T_c$) is remarked by one value of the horizon radius for a high pressure, and two or three horizon radii for low pressure, and the second region ($T > T_c$) is remarked by only one horizon radius, for any value of pressure P . Furthermore, we can see that this van der Waals like behaviour occurs whatever the value of PFDM parameter α .

To get more information about phase transition, we have also studied the heat capacity C , and see how the presence of PFDM and quintessence impact the behaviour of the black hole. This heat capacity is expressed as

$$C = T \left(\frac{\partial S}{\partial T} \right)_{Q,c,\epsilon,P}. \quad (37)$$

Substituting Eqs.(29) and (33) into Eq.(37), we obtain

$$C = \frac{2\pi(Q^3 + r_h^3)^2}{r_h} \left(\frac{A}{B - D} \right), \quad (38)$$

with

$$A = -3r_h^{3\epsilon} \alpha Q^3 \ln\left(\frac{r_h}{\alpha}\right) + r_h^{3\epsilon} \alpha Q^3 - 2r_h^{3\epsilon+1} Q^3 + 3c\epsilon Q^3 + 3r_h^3 c\epsilon + 8\pi P r_h^{3\epsilon+6} + 3cQ^3 + \alpha r^{3\epsilon+3} + r^{3\epsilon+4},$$

$$B = 32\pi P Q^3 r_h^{3\epsilon+6} + 8\pi P r_h^{3\epsilon+9} + 6r_h^{3\epsilon} \alpha Q^6 \ln\left(\frac{r_h}{\alpha}\right) + 15Q^3 \alpha r_h^{3\epsilon+3} \ln\left(\frac{r_h}{\alpha}\right) - 5r_h^{3\epsilon} \alpha Q^6 + 2Q^6 r_h^{3\epsilon+1} - 7Q^3 \alpha r_h^{3\epsilon+3},$$

$$D = 10Q^3 r_h^{3\epsilon+4} - 2\alpha r_h^{3\epsilon+6} - r_h^{3\epsilon+7} - 9Q^6 c\epsilon^2 - 18r_h^3 Q^3 c\epsilon^2 - 9r_h^6 c\epsilon^2 - 15Q^6 c\epsilon - 21r_h^3 Q^3 c\epsilon - 6r_h^6 c\epsilon - 6Q^6 c - 15r_h^3 Q^3 c.$$

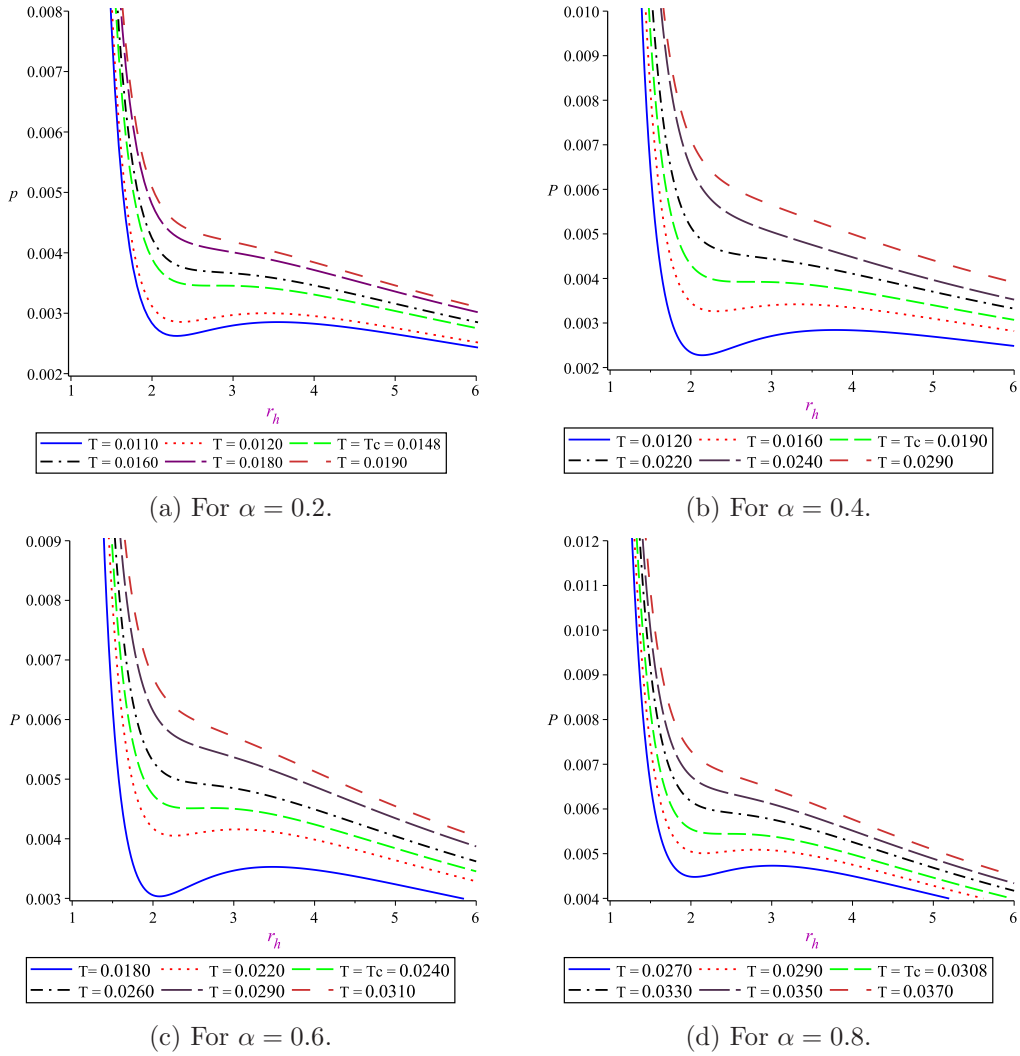
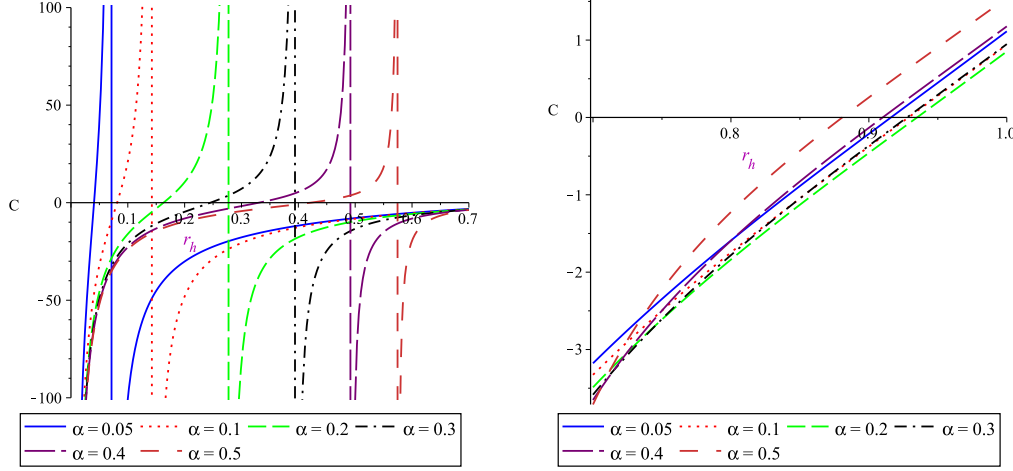


Figure 1. Variation of pressure for different values of α , with $(Q, c, \epsilon) = (1, .2, -2/3)$.

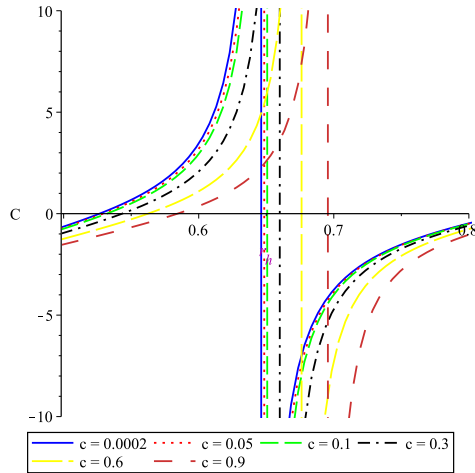
With this in mind, in Fig. 2(a) and (b), the heat capacity is reported for different values of PFDM parameter α . In these plots, it comes that the heat capacity moves from stable phase to unstable one through a second-order phase transition. Here, the unstable phase is remarked by the negative heat capacity($C < 0$), the stable one by the positive heat capacity($C > 0$) and the discontinuity on the plot of heat capacity is identified as the second-order phase transition(see Fig. 2(a) and (c)). Also, notice that this phase transition is shifted towards higher values of the horizon radius as the PFDM parameter increases(see Fig. 2(a)). Furthermore, for higher values of the horizon radius(see Fig. 2(b)), we can see that the heat capacity of the black hole moves from unstable phase to stable phase without any discontinuity, and hence without second-order phase transition. The same behaviour is noticed before the appearance of the phase transition in Fig 2(a).

On the other hand, in order to get more information about the stability of the black hole, in Fig. 2(c) and (d), the heat capacity is plotted for different values of the quintessence parameter c . Analysing these plots, we observe that a second-order phase transition occurs for lower values of the horizon radius. Also, notice that this phase transition is shifted towards higher values of the horizon radius as the quintessence parameter increases. Furthermore for higher values of the horizon radius, the black hole moves from unstable phase to stable phase without second-order phase transition(see Fig. 2(d)).



(a) For smaller values of horizon radius with $(Q, c, \epsilon) = (1, 0.02, -2/3)$.

(b) For higher values of horizon radius with $(Q, c, \epsilon) = (1, 0.02, -2/3)$.



(c) For smaller values of horizon radius with $(Q, \alpha, \epsilon) = (1, 0.6, -2/3)$.

(d) For higher values of horizon radius with $(Q, \alpha, \epsilon) = (1, 0.6, -2/3)$.

Figure 2. Variation of Heat capacity C in term of horizon radius .

Next, let us consider the relationship between the density of PFDM and quintessence in term of α and c , respectively. From Eq. (14), they are expressed as $\rho_{\text{PFDM}} = -\frac{1}{8\pi} \frac{\alpha}{r^3}$ and $\rho_{\text{quint}} = -\frac{3\epsilon c}{2r^3(\epsilon+1)}$. Then we study the impact of them on the behaviour of the black hole. These relations clearly show that the second-order phase transition occurs in the presence of both PFDM and quintessence dark energy, and this phase transition is shifted towards higher values of horizon radius as we decrease the PFDM density and increase the quintessence density.

4 CONCLUSION

In summary, we have studied the thermodynamics of non-linear magnetic-charged black hole surrounded by quintessence in the PFDM background. First, we found the corresponding metric, starting by the action, and then deriving the Einstein-Maxwell equations of motion. Using the energy-momentum tensor of quintessence obtained by Kiselev, and the one for PFDM, used by Zhang *et al.* [82], the metric we found corresponds to the metric obtained by Ma *et al.* [78], for the

quintessence parameter $c = 0$ and cosmological constant $\Lambda = 0$.

Secondly, considering the cosmological constant term Λ as a dynamical pressure, we found the thermodynamic quantities at the horizon radius, namely the mass, temperature, entropy, pressure and the heat capacity. We found that they are affected by the presence of quintessence and PFDM. In particular, for fixed values of quintessence parameters, the critical values of temperature and pressure increase as we increase the PFDM parameter α (see Table 1). Furthermore, our analysis led us to plot the pressure, with respect to the horizon radius. In this plot, we localized two regions, and the presence of a first-order phase transition, which allows us to move from one region to the second one. Indeed, we found a first region ($T < T_c$), remarked by one value of radius for a high pressure, and two or three horizon radii for low pressure, and the second region ($T > T_c$) is remarked by only one horizon radius, for any value of pressure P (see Fig. 1). This behaviour is similar to the van der Waals gas one.

Thirdly, another phase transition we observed is the second-order phase transition, localised in the plot of the heat capacity, with respect to the horizon radius (see Fig. 2). Looking at this the plot, we saw that as we increase PFDM parameter c as well as the quintessence parameter c , the second-order phase transition occurs, and is shifted towards higher values of the horizon radius.

Finally, taking into account the relationship between PFDM and quintessence densities in term of α and c , respectively, we found that the second-order phase transition is shifted towards higher values of the horizon radius as the PFDM density decreases and the quintessence density increases.

References

1. S. W. Hawking, *Nature* **248**, 30 (1974).
2. J. D. Bekenstein, *Phys. Rev. D* **7**, 2333 (1973).
3. J. D. Bekenstein, *Phys. Rev. D* **12**, 3077 (1975).
4. J. D. Bekenstein, *Phys. Rev. D* **7**, 949 (1973).
5. J. M. Bardeen, B. Carter and S. W. Hawking, *Commun. Math. Phys.* **31**, 161 (1973).
6. S. W. Hawking, *Commun. Math. Phys.* **43**, 199 (1975).
7. R. Tharanath and V. C. Kuriakose, *Mod. Phys. Lett. A* **28**, 1350003 (2013).
8. G. W. Gibbons and S. W. Hawking, *Phys. Rev. D* **15**, 2738 (1977).
9. Y.-H. Wei and Z.-H. Chu, *Chinese Phys. Lett.* **28**, 100403 (2011).
10. K. Ghaderi and B. Malakolkalami, *Nuclear Phys. B* **903**, 10, (2016).
11. M. Shahjalal, *Nuclear Phys. B* **940**, 63 (2019).
12. R. Banerjee and D. Roychowdhury, *JHEP* **2011**, 4 (2011).
13. M. Appels, R. Gregory, and D. Kubiznák, *Phys. Rev. Lett.* **117**, 131303 (2016).
14. V. Husain and R. B. Mann, *Class. Quantum Grav.* **26**, 075010 (2009).
15. S. Mahamat, T. Bouetou and T. C. Kofane, *Int. J. of Theo. Phys.* **57**, 2640 (2018).
16. P. C. Davies, *Proceedings of the Royal Society of London. A. Mathematical and Physical Sciences* **353**, 49 (1977).
17. S. Hawking and R. Penrose, *The nature of space and time* (Princeton University Press) (2010).

18. S. Hawking, and G. Ellis, *The large scale structure of space-time* (Cambridge university press) **1**, (1973).
19. J.M. Bardeen, *in: Conference Proceedings of GR5* (Tbilisi, USSR, p. 174) (1968).
20. E. Ayón-Beato and A. García, Phys. Lett. B **493**, 14, (2000).
21. N. Bretón, Phys. Rev. D **72**, 044015 (2005).
22. A. Abdjabbarov, B. Ahmedov and B. Jurayeva, Phys. Rev. D **87**, 064042 (2013).
23. R. Ruffini, Y.-B. Wu and S.-S. Xue, Phys. Rev. D **88**, 085004 (2013).
24. Y.-K. Lim, Phys. Rev. D **91**, 024048 (2015).
25. A. Allahyari, M. Khodadi, S. Vagnozzi and D. Mota, J. Cosmol. Astropart. Phys. **2020**, 003 (2020).
26. A. G. Riess *et al.*, Astronom. J **116**, 1009 (1998).
27. A. G. Riess *et al.*, Astronom. J **117**, 707 (1999).
28. S. J. Perlmutter *et al.*, Astronom. J **517**, 565 (1999).
29. Planck Collaboration (P.A.R. Ade *et al.*), Astron. Astrophys. **571**, A16 (2014).
30. W. Javed, and R. Babar, Advances in High Energy Physics 2019, 2759641 (2019).
31. V. V. Kiselev, Class. Quantum Grav **20**, 1187 (2003).
32. S. B. Chen, B. Wang and R. Su, Phys. Rev. D **77**, 124011 (2008).
33. B. B. Thomas, M. Saleh, and T. C. Kofane, Gen. Rel. and Grav. **44**, 2181 (2012).
34. S. Fernando, Mod. Phys. Lett. A **28**, 1350189 (2013).
35. G.-Q. Li, Phys. Lett. B **735**, 256 (2014).
36. Z. Xu and J. Wang, Phys. Rev. D **95**, 064015 (2017).
37. A. Younas, M. Jamil and S. Hussain, Phys. Rev. D **92**, 084042 (2015).
38. J. de Oliveira and R. Fontana, Phys. Rev. D **98**, 044005 (2018).
39. Z. Xu, X. Hou and J. Wang, Class. and Quantum Grav. **35**, 115003 (2018).
40. J. F. Navarro, C.S. Frenk, S.D.M. White, ApJ **490**, 493 (1997).
41. K. Dutta *et al.*, Phys. Dark U. 100855 (2021).
42. J. A Ruiz, Eur. Phys. J. Plus **136**, 1 (2021).
43. C. Cosme, Catarina, J. Rosab and O. Bertolamia, *Quantum Theory and Symmetries: Proceedings of the 11th International Symposium, Montreal, Canada*(Springer Nature), 417 (2021).
44. L. Padilla *et al.*, The Astrophys J . **909**, 2 (2021).
45. G. Siddhartha, T. Matos, D. Nunez, E. Ramirez, Rev. Mex. Fis. **49**, 203 (2003).
46. K. Saurabh, K and K. Jusufi, Eur. Phys. J. C **81**, 1 (2021).
47. S. Shaymatov, B. Ahmedov and M. Jamil, Eur. Phys. J. C **81**, 1 (2021).
48. M. Ghosh, Mod. Phys. Lett. A **36**, 2150043 (2021).

49. T.-C. Ma et *al.*, Mod. Phys. Lett. A 2150112 (2021).

50. S.W. Hawking, D.N. Page, Commun. Math. Phys. **87**, 577 (1983).

51. N. Farhangkhah and Z. Dayyani, Phy. Rev. D **104**, 024068 (2021).

52. B. Wu *et al.*, Eur. Phys. J. C **81**, 1 (2021).

53. S. Hendi and K. Jafarzade, Phy. Rev. D **103**, 104011 (2021).

54. P. Dolan, Class. and Quantum Grav **28**, 235017 (2011).

55. P. Dolan, Class. and Quantum Grav **28**, 125020 (2011).

56. S. Hendi, A. Nemati K. Lin and M. Jamil, Eur. Phys. J. C **80**, 1 (2020).

57. H. Wei, M. Benrong and T. Jun, Nuclear Phys. B **949**, 114826 (2019).

58. K.-J. He, X.-Y. Hu and X.-X. Zeng, Chinese Phys. C **43**, 125101 (2019).

59. J. Toledo and V. Bezerra, Gen. Rel. and Grav. **52**, 1 (2020).

60. X.-Y. Guo et *al.*, Eur. Phys. J. C **80**, 1(2020).

61. M. Chabab and S. Iraoui, Gen. Rel. and Grav. **52**, 1 (2020).

62. J. Liang, B. Mu and J. Tao, Chinese Phys. C **45**, 023121 (2021).

63. K. K. Rodrigue, M. Saleh, B. B. Thomas and T. C. Kofane, Mod. Phys. Lett. A **35**, 2050129 (2020).

64. R.-G. Cai, L.-M. Cao and N. Ohta, Phys. Lett. B **679**, 504 (2009).

65. K. K. Rodrigue, M. Saleh, B. B. Thomas and T. C. Kofane, Gen. Rel. and Grav. **50**, 52 (2018).

66. R. Tharanath, N.Varghese and V. Kuriakose, Mod. Phys. Lett. A **29**, 1450057 (2014).

67. H.-L. Li and W. Li, Int. J. of Theo. Phys. **59**, 3032 (2020).

68. C. H. Nam, Gen. Rel. and Grav. **50**, 57 (2018).

69. G.-Q. Li and S.-F. Xiao, Phy. Rev. D **86**, 123015 (2012).

70. Z. Xu, X. Hou, J. Wang and Y. Liao, Adv High Energy Phys. 2019 (2019).

71. J. Sadeghi, E. Mezerji and S. Gashti, arXiv:2011.14366 (2020).

72. H. Salazar, A. García and J. Plebanski, J. Math. Phys. **28**, 2171 (1987).

73. M. Novello, S. Bergliaffa, and J. Salim, Class. Quantum Grav. **17**, 3821 (2000).

74. C. H. Nam, Gen. Rel. and Grav. **52**, 1 (2020).

75. C. H. Nam, Eur. Phys. J. C **78**, 418 (2018).

76. R.T. Ndongmo, S. Mahamat, T.B. Bouetou, T.C. Kofane. Phys. Scr. **96**, 095001 (2021).

77. Y. Chen et *al.*, arXiv:2009.03778 (2020).

78. T.-C. Ma et *al.*, arXiv:2010.00151 (2020).

79. M. Sadeghi, arXiv:2007.09688 (2020).

80. S. Ghosh et *al.*, Eur. Phys. J. C **78**, 1 (2018).
81. C. Böhmer, N. Tamanini and M. Wright, Phys. Rev. D **91**, 123002 (2015).
82. H.-X. Zhang et *al.*, Chinese Phys. C (2021).
83. C. Rizwan, A. Kumara, K. Hegde and D. Vaid, arXiv:2008.06472 (2020).